Modeling Viscoelastic Dielectrics

Wei Hong
Department of Aerospace Engineering, Iowa State University, Ames, IA 50011, USA

Abstract

Dielectric elastomer, as an important category of electroactive polymers, is known to have viscoelastic properties that strongly affect its dynamic performance and limit its application. Very few models accounting for the effects of both electrostatics and viscoelasticity exist in the literature, and even fewer are capable of making reliable predictions under general loads and constraints. Based on the principals of nonequilibrium thermodynamics, this paper develops a field theory that fully couples the large inelastic deformations and electric fields in deformable dielectrics. Our theory recovers existing models of elastic dielectrics in the equilibrium limit. This paper proposes, in a general nonequilibrium state, the mechanism of instantaneous instability which corresponds to the pull-in instability often observed on dielectric elastomers. Most finite-deformation constitutive relations and evolution laws of viscoelastic solids can be directly adopted in the current theoretical framework. As an example, a specific material model is selected and applied to the uniform deformation of a dielectric elastomer. This model predicts the stability criteria of viscoelastic dielectrics and its dependence on loading rate and the effect of pre-stress and relaxation. The dynamic response and the hysteresis behavior of a viscoelastic dielectric elastomer under cyclic electric fields are also studied.

Keywords: Dielectric elastomer; Viscoelasticity; Large deformation; Piezoelectricity

whong@iastate.edu

1 Introduction

Electroactive polymers, as a category of polymeric materials that deform under electrical stimuli, are emerging as promising alternatives to existing materials for actuation and sensing applications. In contrast to traditional actuator materials (e.g. piezoelectric ceramics) which are known for their high load capacity but small deformation, electroactive polymers are characterized by their softness, flexibility, and the consequent large-deformation capability, as reviewed by Bar-Cohen and Zhang (2008). The properties of electroactive polymers resemble those of natural biological muscles, and are expected to provide biomimetic opportunities for industry and bring impact to various areas that include robotics, biomedical devices, and energy harvesting (Bar-Cohen, 2002, 2004; Zhang et al., 2005; Wingert et al, 2006; Sugiyama and Hirai, 2006). Among various types of electroactive polymers, dielectric elastomers are known for their ease of use, high coupling efficiency, light weight, cost effectiveness, and large scope of applications (Kornbluh et al., 1995; Pelrine et al., 1998; Carpi et al., 2008).

A common design of dielectric elastomer film is sketched in Fig. 1. An electric field is applied through the thickness by a pair of electrodes attached to both surfaces of the film. Although rigid plates are used as electrodes in some designs (Lau et al., 2006), stretchable electrodes are commonly used to

accommodate the large in-plane deformation of the elastomer. Just as in a parallel capacitor, charge accumulates on both electrodes upon application of the voltage. The electrostatic attraction between the two oppositely charged electrodes, together with the polarization-induced intrinsic deformation of the material (often referred to as the electrostriction), causes a dielectric elastomer to change in thickness and lateral dimensions. Although the two effects are dissimilar in physical origins, it is practically difficult to measure them separately through experiments, neither is it necessary to distinguish between the two effects for characterizing a dielectric solid (Rinaldi and Brenner, 2002; McMeeking and Landis, 2005; Suo et al., 2008). To prevent buckling or wrinkles, it is preferred that a free-standing dielectric-elastomer film is under tension throughout the entire actuation process, and thus a lateral pre-stretch is usually applied in actuator designs. In addition to the tension needed for free-standing films, pre-stretch is also believed to have a tremendous enhancement to the actuation performance of a dielectric elastomer (Pelrine et al., 2000a, 2000b; Kofod et al. 2003; Zhao et al, 2007a ; Kofod, 2008).

The demand for a theoretical guidance for reliable designs has drawn continuous efforts on modeling the coupling behaviors of dielectric elastomers. Early analyses tend to simplify the material as linear elastic by neglecting the effect of finite deformation, and account for the electromechanical coupling by adding an empirical Maxwell stress (Kornbluh et al., 1995; Pelrine et al., 1998). While these approaches may explain some experimental phenomena, the physical origin remains unclear and the predictions are far from accurate. Later models use a similar approach by employing hyperelastic constitutive laws to a uniformly deformed elastomer and have achieved a better agreement with experiment in some cases (e.g. Pelrine et al., 2000c; Goulbourne et al., 2005; Wissler and Mazza, 2005a). With the more recent development of fully coupled nonlinear field theories (Dorfmann and Ogden, 2005; McMeeking and Landis, 2005; Suo et al., 2008), the mechanism of phenomena such as the pull-in instability are rigorously modeled and predicted (Zhao et al, 2007a; Zhao and Suo, 2007b). It has also been shown that the empirical Maxwell stress only represents the behavior of a special class of materials that possess no physical electromechanical coupling (Zhao et al, 2007a), and therefore may not be applicable to some other dielectric elastomers (Zhao and Suo, 2008a, 2009). The framework of the nonlinear field theory has yielded various finite-element implementations that further enable numerical simulation of dielectric elastomers under complex working conditions (Zhou et al., 2008; Zhao and Suo, 2008b).

It has long been realized through experiments that the electromechanical responses of dielectric elastomers are highly rate-dependent (Pelrine et al., 2000a; Zhang et al., 2005; Plante and Dubowsky, 2006), implying that the mechanical property of dielectric elastomers may be viscoelastic. The rate-dependency of a dielectric elastomer can influence its dynamic performance and coupling efficiency (Kornbluh et al., 2000), and thus limit its application. However, very few researches have been carried out on modeling the electro-viscoelastic properties of dielectric elastomers. Some early approaches use linear viscoleasticity to model relatively small deformations (e.g. Yang et al., 2005; Wissler and Mazza, 2005b). Recently, Plante and Dubowsky (2007) studied the dynamic performance of dielectric elastomers using a modified Bergström-Boyce model (1998) for the finite-deformation viscoelasticity,

and achieved good agreement with experimental results. These models either consider solely the mechanical behavior of dielectric elastomer, or treat the electromechanical coupling by adding the Maxwell stress. Many questions remain unclear even with all these models developed. For example, how accurate would the Maxwell-stress approach be for real materials, especially those with significant electrostriction effects? Should the added Maxwell stress only appear in the elastic response of the material, or should it affect the inelastic deformation as well? How would a material model be verified by experiments and how can one calibrate it for a specific material?

To answer at least some of these questions, we aim at developing a continuum field theory for the behavior of a viscoelastic dielectric under combined electric and mechanical loads. Following the approach previously taken by Suo et al. (2008) in developing the field theory for elastic dielctrics, we only use measurable quantities such as mechanical forces and electric potential to define field variables. In Section 2, we define the fields of stress and electric displacement by using virtual work, or equivalently, the momentum balance and Gauss's law of electrostatics. Such definitions avoid the ambiguity when physical quantities are defined using material laws, especially in nonequilibrium cases. The virtual-work-based definitions further ease the introduction of the thermodynamic principles in Section 3, where general guidelines for the material laws of viscoelastic dielectrics are derived for the first time. As another emphasis of the paper, Section 4 discusses the stability of a viscoelastic dielectric in a nonequilibrium state, and introduces the idea of instantaneous instability which corresponds to an important failure mode of dielectric elastomers. Under some physical assumptions, Section 5 proposes a simplest material law for viscoelastic dielectrics, and Section 6 uses it to analyze the homogeneous deformation and stability of a dielectric-elastomer film as an illustrative example for the usage of the theory.

2 Definition of the fields

Although any state of a material may serve as a reference state, here for simplicity, we take a fully relaxed state as the reference, in which the material is under no external electrical or mechanical load. Following the usual practice in finite-deformation solid mechanics, we identify a material particle by its position vector in the reference state, $\mathbf{X}$, and trace its motion by the current position at time t, $\mathbf{x}(\mathbf{X},t)$. At least in a state of thermodynamic equilibrium, the local information on the deformation and rotation of a material particle is characterized by the deformation gradient tensor,

$$F_{iK} = \frac{\partial x_i(\mathbf{X},t)}{\partial X_K}. \tag{1}$$

While the definitions of internal fields such as stress can be ambiguous especially when the system is not in equilibrium, we simply define them as the internal representatives of externally applied loads, independent of the material properties and the thermodynamic state. The definitions of stress and electric displacement given below closely follow those in an equilibrium state by Suo et al. (2008). In the reference state, let $dV(\mathbf{X})$ be the volume of a material particle, and $dA(\mathbf{X})$ be the area of a material element on a surface. Correspondingly, we denote the mechanical force in the volume as

$\mathbf{b}(\mathbf{X},t)dV$ and that on the surface as $\mathbf{t}(\mathbf{X},t)dA$. We define the tensor of nominal stress (i.e. the Piola-Kirchhoff stress of the first kind), $\mathbf{P}(\mathbf{X},t)$, such that the equation

$$\int_{\Omega} P_{iK}\frac{\partial \xi_i}{\partial X_K}dV = \int_{\Omega} b_i\xi_i dV + \int_{\partial\Omega} t_i\xi_i dA \tag{2}$$

holds true for arbitrary field $\boldsymbol{\xi}(\mathbf{X})$ in any domain Ω and on its surface $\partial\Omega$. Inertial forces are neglected in the current paper. While Eq. (2) is only a definition of the stress field and the vectorial test function $\boldsymbol{\xi}(\mathbf{X})$ needs no physical interpretation, Eq. (2) becomes the principal of virtual work when $\boldsymbol{\xi}$ is taken to be a virtual displacement field, and the stress defined here recovers the common definition in a state of thermodynamic equilibrium.

Applying the divergence theorem to the left-hand side of Eq. (2), through integration by parts, one would easily obtain a mathematically equivalent definition of the nominal stress:

$$\frac{\partial P_{iK}}{\partial X_K} + b_i = 0 \tag{3}$$

in the volume of the body and

$$\left(P_{iK}^{-} - P_{iK}^{+}\right)N_K = t_i \tag{4}$$

on an interface where the mechanical traction $\mathbf{t}$ is applied. The labels "+" and "–" differentiate the media on the two sides of the interface. The unit vector $\mathbf{N}$ is normal to the interface in the reference state, pointing towards the medium "+". Eqs. (3) and (4) do not imply equilibrium of the system, but serve merely as the definition of stress, just as Eq. (2).

At time t, the material particle $\mathbf{X}$ has electric potential $\Phi(\mathbf{X},t)$. The nominal electric field is defined as the gradient of the electric potential with respect to the reference state:

$$\widetilde{E}_K = \frac{\partial\Phi(\mathbf{X},t)}{\partial X_K}. \tag{5}$$

In the current state, let the charge in a volume element of material be $\tilde{q}(\mathbf{X},t)dV$ and that on a surface element be $\tilde{\omega}(\mathbf{X},t)dA$. Similar as the nominal electric field and the mechanical body and surface loads, the charge densities $\tilde{q}$ and $\tilde{\omega}$ are both measured with respect to the geometry in the reference. We define the vector field of nominal electric displacement, $\widetilde{\mathbf{D}}(\mathbf{X},t)$, such that

$$\int_{\Omega}\left(-\frac{\partial\eta}{\partial X_K}\right)\widetilde{D}_K dV = \int_{\Omega}\eta\tilde{q}dV + \int_{\partial\Omega}\eta\tilde{\omega}dA \tag{6}$$

holds true for arbitrary test function $\eta(\mathbf{X})$. Upon application of the divergence theorem, Eq. (6) yields an equivalent definition of the nominal electric displacement in a differential form:

$$\frac{\partial \tilde{D}_K}{\partial X_K} = \tilde{q} \tag{7}$$

in the volume and

$$\left(\tilde{D}_K^- - \tilde{D}_K^+\right) N_K = \tilde{\omega} \tag{8}$$

on the surface. In an equilibrium state, Eqs. (7) and (8) are known as Gauss's law of electrostatics.

Due to the soft nature of the material, large deformation is usually expected and the geometries in the current and reference states differ significantly. The quantities defined here are nominal fields in a Lagrange description. When needed, equations in terms of the nominal quantities can be easily rewritten in the current state using the geometric relations between the nominal and true fields, such as

$$\sigma_{ij} = \frac{P_{iK} F_{jK}}{\det \mathbf{F}},\ D_i = \frac{\tilde{D}_K F_{iK}}{\det \mathbf{F}}, \text{ and } E_i F_{iK} = \tilde{E}_K, \tag{9}$$

where $\boldsymbol{\sigma}$, $\mathbf{D}$, and $\mathbf{E}$ are the true stress, true electric displacement, and the true electric field, respectively.

3 Nonequilibrium thermodynamics

Consider a body of deformable dielectrics, loaded mechanically by a field of body force $\mathbf{b}$ and surface traction $\mathbf{t}$, and electrically by a field of batteries with electric potential Φ. Associated with a displacement field $\delta\mathbf{x}$ and change in the nominal charge densities $\delta\tilde{q}$ and $\delta\tilde{\omega}$, the external electrical and mechanical loads do work

$$\int b_i \delta x_i dV + \int t_i \delta x_i dA + \int \Phi \delta \tilde{q} dV + \int \Phi \delta \tilde{\omega} dA. \tag{10}$$

Let W be the Helmholtz free energy of the material per unit reference volume, and δW be its change associated with the displacement and charge redistribution. Utilizing the definition of stress and electric displacement, one has the corresponding change in the total free energy of the system, G, including the potential of the external loads,

$$\delta G = \int \left(\delta W - P_{iK} \delta F_{iK} - \tilde{E}_K \delta \tilde{D}_K\right) dV. \tag{11}$$

The laws of thermodynamics dictate that the free energy of the system never increases, $\delta G \le 0$. For the change in displacement and change distribution to be physically possible, the inequality must hold true in any volume. Therefore, we have

$$\delta W - P_{iK}\delta F_{iK} - \tilde{E}_K \delta \tilde{D}_K \le 0 . \tag{12}$$

Inequality (12) holds true on any material particle for any process, and the equal sign takes place only when the process is reversible, i.e. the system is locally in equilibrium. The thermodynamic equilibrium state of a material particle is fully determined by the deformation gradient and the electric displacement. For a general inelastic material, the free energy in a nonequilibrium state differs from that in an equilibrium state. To distinguish between them, we introduce the equilibrium Helmholtz free-energy density, and write it as $W^{EQ}\left(\mathbf{F},\tilde{\mathbf{D}}\right)$. From (12) in the case of an equal sign, we obtain the following constitutive relations in an equilibrium state:

$$P_{iK}^{EQ}\left(\mathbf{F},\tilde{\mathbf{D}}\right)=\frac{\partial W^{EQ}\left(\mathbf{F},\tilde{\mathbf{D}}\right)}{\partial F_{iK}},\ \tilde{E}_K^{EQ}\left(\mathbf{F},\tilde{\mathbf{D}}\right)=\frac{\partial W^{EQ}\left(\mathbf{F},\tilde{\mathbf{D}}\right)}{\partial \tilde{D}_K}, \tag{13}$$

in which $\mathbf{P}^{EQ}$ and $\tilde{\mathbf{E}}^{EQ}$ are the nominal stress and the nominal electric field in an equilibrium state.

To describe a non-equilibrium state, following the usual approach in finite-deformation viscoelasticity and plasticity (Lee, 1969), we imagine an intermediate state between the reference state and the current state, which may be achieved physically by isolating and elastically relaxing the material particle. Denoting the deformation gradient of the intermediate state as $\mathbf{F}^i\left(\mathbf{X},t\right)$, and that of the current state with respect to the intermediate state as $\mathbf{F}^e\left(\mathbf{X},t\right)$, we have the multiplicative decomposition of the deformation gradient:

$$F_{iK} = F^e_{ij'}F^i_{j'K} . \tag{14}$$

For clarity, the indices corresponding to the coordinates in the intermediate state are primed. The electric fields, on the other hand, equilibrate much faster than mechanical deformations. In the regime where most dielectric elastomers are applied, it is safe to assume that the electric fields are always in equilibrium, $\tilde{\mathbf{E}} \equiv \tilde{\mathbf{E}}^{EQ}$.

Following Reese and Govindjee (1998), we assume that the non-equilibrium Helmholtz energy, namely the difference between the Helmholtz free energy of a non-relaxed state and that of an equilibrium state, depends only on the elastic deformation between the relaxed intermediate state and the current state

$$W - W^{EQ} \equiv W^{NEQ}\left(\mathbf{F}^e\right). \tag{15}$$

Since the irreversible deformation in the intermediate state is more suitable in characterizing the non-equilibrium state of the material, here we take the corresponding deformation gradient $\mathbf{F}^i$ as an internal state variable, and write the total Helmholtz free energy density as

$$W\left(\mathbf{F},\mathbf{F}^i,\tilde{\mathbf{D}}\right)=W^{EQ}\left(\mathbf{F},\tilde{\mathbf{D}}\right)+W^{NEQ}\left(\mathbf{F}\cdot\mathbf{H}^i\right), \tag{16}$$

where $\mathbf{H}^i$ is the inverse tensor of the deformation gradient of the intermediate state, $\mathbf{H}^i = \left(\mathbf{F}^i\right)^{-1}$. Due to the electrostatic equilibrium assumption, the nominal electric displacement does not appear in the non-equilibrium free-energy function W^{NEQ}.

Substituting Eqs. (13) and (16) into the thermodynamic inequality (12), one arrives at

$$\left(P_{jK} - \frac{\partial W}{\partial F_{jK}}\right)\delta F_{jK} - \frac{\partial W}{\partial F^i_{l'K}}\delta F^i_{l'K} \geq 0\,. \tag{17}$$

Inequality (17) holds true for arbitrary physically possible processes away from the current state, described by $\delta\mathbf{F}$ and $\delta\mathbf{F}^i$, including reversible processes in which an equal sign should be taken. Therefore, the nominal stress is the derivative of the Helmholtz free-energy density with respect to the deformation gradient even in a non-equilibrium state (Coleman and Gurtin, 1967),

$$P_{jK} = \frac{\partial W}{\partial F_{jK}} = P^{EQ}_{jK} + P^{NEQ}_{jm'}H^i_{Km'}\,, \tag{18}$$

where the inelastic nominal stress tensor $\mathbf{P}^{NEQ}$ is given by

$$P^{NEQ}_{jm'} = \frac{\partial W^{NEQ}}{\partial F^e_{jm'}}. \tag{19}$$

The remainder of the inequality that governs the evolution of the inelastic internal variables becomes:

$$P^{NEQ}_{jm'}F^e_{jl'}H^i_{Km'}\delta F^i_{l'K} \geq 0\,, \tag{20}$$

which physically indicates that the energy of the system only dissipates in inelastic deformation.

Since the behavior of viscoelastic materials are usually rate-dependent, it is often more useful to replace the variation expressions by the corresponding rates of change, e.g. $\dot{\mathbf{F}}^i = \delta\mathbf{F}^i \big/ \delta t$. If we further introduce the inelastic true stress

$$\sigma^{NEQ}_{ij} = \frac{P^{NEQ}_{im'}F^e_{jm'}}{\det\mathbf{F}^e}\,, \tag{21}$$

we can rewrite inequality (20) in the current configuration as:

$$\sigma^{NEQ}_{mn}L^i_{mn} \geq 0\,, \tag{22}$$

where $\mathbf{L}^i$ is the inelastic part of the covariant velocity gradient

$$L_{mn} = \dot{F}_{mK} H_{Kn} = L^e_{mn} + L^i_{mn} = \dot{F}^e_{mj'} H^e_{j'n} + F^e_{mj'} \dot{F}^i_{j'K} H^i_{Kp'} H^e_{p'n} . \tag{23}$$

Here $\mathbf{H}$ and $\mathbf{H}^e$ are the inverses of the corresponding deformation gradient tensors. Due to the symmetry of the true stress tensor, inequality (22) is sometimes written in terms of the symmetric part of the inelastic velocity gradient, i.e. the inelastic stretch rate $\mathbf{Q}^i = \left(\mathbf{L}^i + \mathbf{L}^{i^T}\right)/2$,

$$\sigma^{NEQ}_{mn} Q^i_{mn} \geq 0 . \tag{24}$$

While inequality (24) as a consequence of the second law of thermodynamics must be satisfied by all processes for any material, a kinetic evolution equation in the form

$$Q^i_{jk} = M_{jkmn} \sigma^{NEQ}_{mn} \tag{25}$$

is often used in practice. The forth-rank mobility tensor $\mathbf{M}$ is material-dependent and is always positive-definite so that inequality (24) is satisfied automatically. In general models for the evolution of internal parameters, the mobility tensor may be dependent on various state variables as well. Equations (13), (18) and (25), together with the definition of state variables in Section 2, form a closed system for the analysis of the coupled electromechanical response of viscoelastic dielectrics. It is noteworthy that the evolution of the inelastic deformation is not fully determined, since Eq. (25) contains no information on rotation. The inelastic deformation can be made unique through various ways, and the choice of approach is not essential as demonstrated by Boyce et al. (1989). One convenient way is to simply discard rotation in the intermediate state.

4 Instabilities in viscoleastic dielectric elastomers

Among various applications of dielectric elastomers, one major mode of failure is induced by electromechanical instability (e.g. Stark and Garton, 1955; Blok and LeGrand, 1969; Zeller and Schneider, 1984; Plante and Dubowsky, 2006). Let us first look at the stability of a thermodynamic equilibrium state. Under the currently developed framework, to reach a true thermodynamic equilibrium state, the material must be fully relaxed, and no inelastic deformation is underway, $\mathbf{L}^i = \mathbf{0}$. Therefore, in a state of equilibrium, the inelastic stress vanish $\mathbf{P}^{NEQ} = \mathbf{0}$, and the system is identical to that of an elastic dielectrics (Suo et al., 2008). An equilibrium state is stable when the total free energy of the system reaches a local minimum. In a system where constant loads and voltages are applied, a state is stable when the equilibrium Hessian

$$\aleph^{EQ} = \begin{bmatrix} \dfrac{\partial W^{EQ}\left(\mathbf{F}, \tilde{\mathbf{D}}\right)}{\partial F_{iK} \partial F_{jL}} H_{Pi} H_{Qj} & \dfrac{\partial W^{EQ}\left(\mathbf{F}, \tilde{\mathbf{D}}\right)}{\partial F_{iK} \partial \tilde{D}_M} H_{Pi} \\ \dfrac{\partial W^{EQ}\left(\mathbf{F}, \tilde{\mathbf{D}}\right)}{\partial F_{jL} \partial \tilde{D}_N} H_{Qi} & \dfrac{\partial W^{EQ}\left(\mathbf{F}, \tilde{\mathbf{D}}\right)}{\partial \tilde{D}_M \partial \tilde{D}_N} \end{bmatrix} \tag{26}$$

is positive-definite. All indices in Eq. (26) are pulled back to the reference state to exhibit the implied symmetry, and the four entries in the matrix represent sub matrices. The stability of an elastic dielectric has already been studied extensively (e.g. Zhao et al. 2007a; Zhao and Suo 2007b, 2009), and here we will look at another type of instabilities specifically for viscoelastic materials.

It may seem peculiar to talk about the stability of a nonequilibrium state, but phenomena similar to the instability of an equilibrium state have been observed experimentally in viscoelastic materials (Plante and Dubowsky, 2006). The failure induced by these phenomena is often catastrophic, and takes place at a state far from the fully-relaxed equilibrium state. Moreover, the occurrence of these phenomena is dependent on the loading rate. Inspired from the fact that these phenomena complete much faster than the relaxation processes, we propose the following mechanism. At a time scale much shorter than the characteristic time of the evolution of inelastic deformation, the system may be regarded as in a state of equilibrium. If any perturbation on the state variables other than the viscoelastic internal variable will lower the total free energy of the current state, the state is likely to be driven away dynamically, since the rate-dependent dissipative process is assumed to be inactive. To distinguish from the common idea of stability, we will refer to such phenomena as *instantaneous instabilities*.

Similar as equilibrium states, a non-equilibrium state is *instantaneously stable* when the total free energy of the system increases upon any instantaneous change in the deformation and charge density. In other words, the free energy of the system is minimized on the hypersurface spanned by $\mathbf{F}$ and $\tilde{\mathbf{D}}$, when $\mathbf{F}^i$ is held constant, in the hyperspace of states $\left(\mathbf{F},\mathbf{F}^i,\tilde{\mathbf{D}}\right)$. Specifically, in a system of force- and voltage-controlled loads, the critical condition for an *instantaneous instability* is that the Hessian

$$\aleph\left(\mathbf{F},\mathbf{F}^i,\tilde{\mathbf{D}}\right)=\begin{bmatrix} \dfrac{\partial W\left(\mathbf{F},\mathbf{F}^i,\tilde{\mathbf{D}}\right)}{\partial F_{iK}\partial F_{jL}}H_{Pi}H_{Qj} & \dfrac{\partial W\left(\mathbf{F},\mathbf{F}^i,\tilde{\mathbf{D}}\right)}{\partial F_{iK}\partial \tilde{D}_M}H_{Pi} \\ \dfrac{\partial W\left(\mathbf{F},\mathbf{F}^i,\tilde{\mathbf{D}}\right)}{\partial F_{jL}\partial \tilde{D}_N}H_{Qi} & \dfrac{\partial W\left(\mathbf{F},\mathbf{F}^i,\tilde{\mathbf{D}}\right)}{\partial \tilde{D}_M\partial \tilde{D}_N} \end{bmatrix} \tag{27}$$

becomes singular, $\det\aleph=0$.

The physical significance of the instantaneous stability of a nonequilibrium state would be clearer if we refer to the rate form of governing equations. Taking material derivatives on both sides of Eqs. (13) and (18) and utilize the symmetry, we have

$$\begin{cases} \dot{P}_{jK} = \dfrac{\partial^2 W}{\partial F_{jK}\partial F_{mN}}\dot{F}_{mN} + \dfrac{\partial^2 W}{\partial F_{jK}\partial \widetilde{D}_N}\dot{\widetilde{D}}_N + \dfrac{\partial^2 W}{\partial F_{jK}\partial F^i_{mN}}\dot{F}^i_{mN} \\ \dot{\widetilde{E}}_K = \dfrac{\partial^2 W}{\partial \widetilde{D}_K\partial F_{mN}}\dot{F}_{mN} + \dfrac{\partial^2 W}{\partial \widetilde{D}_K\partial \widetilde{D}_N}\dot{\widetilde{D}}_N + \dfrac{\partial^2 W}{\partial \widetilde{D}_K\partial F^i_{mN}}\dot{F}^i_{mN} \\ \sigma^{NEQ}_{mn} = M^{-1}_{mnjk}Q^i_{jk} \end{cases} . \tag{28}$$

The rates of evolution $\dot{\mathbf{F}}$, $\dot{\widetilde{\mathbf{D}}}$ and $\dot{\mathbf{F}}^i$ can be determined when the coefficient matrix of the right-hand side of system (28) is nonsingular. Similar to the criterion of deformation localization during plastic deformation (Rice, 1976), the critical condition for unstable evolution is the singularity of the coefficient matrix. Since the mobility tensor $\mathbf{M}$ is positive-definite, the critical condition for instability is reduced to the singularity of the Hessian, $\det \aleph = 0$, identical to the condition of instantaneous instability described above.

5 A specific material model

To apply the nonlinear field theory developed in preceding sections to the analysis of dielectric elastomers, one needs to specify the Helmholtz free-energy functions $W^{EQ}\left(\mathbf{F},\widetilde{\mathbf{D}}\right)$ and $W^{NEQ}\left(\mathbf{F}^e\right)$, as well as the mobility tensor $\mathbf{M}$. In order to characterize the material behavior under various loading conditions, during the past decades, there has been continuous effort on developing equilibrium models (e.g. James and Guth, 1943; Treloar, 1975; Flory, 1977; Arruda and Boyce, 1993) and kinetic evolution models (e.g. Lubliner, 1985; Haupt, 1993; Reese and Govindjee, 1998; Bergström and Boyce, 1998) for polymeric materials in absence of external electric field. Possible forms of the equilibrium free-energy function $W^{EQ}\left(\mathbf{F},\widetilde{\mathbf{D}}\right)$ that couples electric field and deformation have also been studied recently (e.g Dorfmann and Ogden, 2006; Zhao et al., 2007a; Zhao and Suo, 2008a; Richards and Odegard, 2010). When a combination of specific material laws are selected, the field theory presented here recovers the model developed by Plante and Dubowsky (2007). For quantitative prediction of a specific type of dielectric elastomers, the readers are suggested to select suitable free-energy functions and mobility in the literature, and calibrate the models using experimental data. Here for the purpose of demonstration, we will construct the simplest model possible to qualitatively study some phenomena.

Following Zhao et al. (2007a), we assume the material behaves in equilibrium as an ideal dielectric elastomer, of which the free-energy density only consists of the contributions from stretching and polarization $W^{EQ}\left(\mathbf{F},\widetilde{\mathbf{D}}\right) = W_s^{EQ}\left(\mathbf{F}\right) + W_p\left(\mathbf{D}\right)$. The physical decoupling between the deformation and the true electric displacement represents a category of materials that have liquid-like polarization behavior independent of the deformation state. For simplicity, we further assume the dielectric property to be linear and the free energy of stretching to be entropic with Gaussian statistics (Treloar, 1975), so that the equilibrium free-energy function reads

$$W^{EQ}\left(\mathbf{F},\tilde{\mathbf{D}}\right)=\frac{\mu^{EQ}}{2}F_{iK}F_{iK}+\frac{D_iD_i}{2\varepsilon}=\frac{\mu^{EQ}}{2}F_{iK}F_{iK}+\frac{1}{2\varepsilon}F_{iK}\tilde{D}_K\tilde{D}_NF_{iN}\,, \tag{29}$$

where μ^{EQ} is the equilibrium or long-term modulus, and ε is the dielectric permittivity. Similarly, we assume the non-equilibrium free-energy function in the form

$$W^{NEQ}\left(\mathbf{F}^e\right)=\frac{\mu^{NEQ}}{2}F^e_{im'}F^e_{im'}=\frac{\mu^{NEQ}}{2}F_{iK}H^i_{Km'}H^i_{Nm'}F_{iN} \tag{30}$$

with non-equilibrium modulus μ^{NEQ}. In the current paper, the material is assumed to be incompressible, with both elastic and inelastic deformations being volume-conservative, $\det\mathbf{F}=\det\mathbf{F}^i=\det\mathbf{F}^e=1$.

Applying the free-energy functions (29) and (30) to Eqs. (13) and (18), we have the following constitutive relations:

$$P_{iK}\left(\mathbf{F},\mathbf{F}^i,\tilde{\mathbf{D}}\right)=\mu^{EQ}F_{iK}+\mu^{NEQ}H^i_{Km'}H^i_{Nm'}F_{iN}+\frac{1}{\varepsilon}\tilde{D}_K\tilde{D}_NF_{iN}-pH_{Ki}\,, \tag{31a}$$

$$\tilde{E}_K\left(\mathbf{F},\tilde{\mathbf{D}}\right)=\frac{1}{\varepsilon}\tilde{D}_NF_{iN}F_{iK}\,, \tag{31b}$$

where p is an undetermined hydrostatic pressure introduced by the incompressibility constraint. Alternatively, the constitutive relation may also be expressed in terms of true quantities:

$$\sigma_{ij}=\mu^{EQ}F_{iK}F_{jK}+\mu^{NEQ}F_{iN}H^i_{Nm'}H^i_{Km'}F_{jK}+\frac{1}{\varepsilon}D_iD_j-p\delta_{ij}\,,\ E_i=\frac{D_i}{\varepsilon}\,. \tag{32}$$

The third term on the right-hand side of Eq. (32), D_iD_j/ε, is usually referred to as the Maxwell stress. This form of the electrostatic contribution to stress is the consequence of a specific free-energy function, and should not be generalized to all materials. Under the current assumption that the polarization of the material is always in equilibrium, an electrostatic contribution does not appear in the inelastic stress $\mathbf{P}^{NEQ}$ or $\boldsymbol{\sigma}^{NEQ}$.

To specify the evolution law for the inelastic deformation, we assume the viscous property of the material to be isotropic in the current state, so that the mobility takes the form

$$M_{ijkl}=\frac{1}{2\eta}\left(\delta_{ik}\delta_{jl}+\delta_{il}\delta_{jk}-\frac{2}{3}\delta_{ij}\delta_{kl}\right). \tag{33}$$

When a constant viscosity η is used, the inelastic behavior of the material resembles that of Newtonian fluid.

6 Homogeneous deformation of a dielectric elastomer film

In this section, we will study the response of a viscoelastic dielectric to applied electric fields, as an example of the theoretical framework developed in the current paper. The material is in the form of a thin film, which has been most widely used in applications. Let λ_1 and λ_2 be the two principal in-plane stretches of the film, and P_1 and P_2 be the nominal stresses applied in the corresponding directions, as depicted in Fig. 1. Due to volume incompressibility, the stretch in the thickness direction is $\lambda_1^{-1}\lambda_2^{-1}$. We assume that the loading direction has not changed in the history, so that the principal directions of the inelastic stretches coincide with those of total stretches, and we will denote the principal inelastic stretches as λ_1^i and λ_2^i. The external electric field $\tilde{E}$ is only applied through the thickness. For simplicity, we assume the deformation to be homogeneous. Therefore, the nominal electric displacement $\tilde{D}$ is also in the thickness direction. The critical condition for instability obtained under a homogeneous assumption is expected to be the upper bound of actual cases when inhomogeneous deformation is allowed.

To simplify mathematical expressions, we introduce the following dimensionless field variables:

$$\overline{P}_1 = \frac{P_1}{\mu},\ \overline{P}_2 = \frac{P_2}{\mu},\ \overline{D} = \frac{\tilde{D}}{\sqrt{\mu\varepsilon}},\ \text{and}\ \overline{E} = \tilde{E}\sqrt{\frac{\varepsilon}{\mu}}, \tag{34}$$

where $\mu = \mu^{EQ} + \mu^{NEQ}$ is the instantaneous modulus of the material.

6.1 Instantaneous instability

Adopting the simple material model constructed in Section 5, we write the dimensionless free-energy density as

$$\frac{W}{\mu}\left(\lambda_1,\lambda_2,\lambda_1^i,\lambda_2^i,\overline{D}\right) = \frac{\chi}{2}\left(\lambda_1^2+\lambda_2^2+\frac{1}{\lambda_1^2\lambda_2^2}\right)+\frac{1-\chi}{2}\left[\left(\frac{\lambda_1}{\lambda_1^i}\right)^2+\left(\frac{\lambda_2}{\lambda_2^i}\right)^2+\left(\frac{\lambda_1^i\lambda_2^i}{\lambda_1\lambda_2}\right)^2\right]+\frac{\overline{D}^2}{2\lambda_1^2\lambda_2^2}. \tag{35}$$

where $\chi = \mu^{EQ}/\mu$ is the ratio between the equilibrium and instantaneous moduli. The material parameter χ physically represents the fraction of the polymer network that has time-independent deformation (Bergström and Boyce, 1998). The material is purely elastic when $\chi = 1$, and becomes a viscous fluid when $\chi = 0$.

The constitutive relations (31) specialize to

$$\overline{P}_1 = \lambda_1\left(\chi+\frac{1-\chi}{{\lambda_1^i}^2}\right)-\frac{1}{\lambda_1^3\lambda_2^2}\left[\chi+(1-\chi){\lambda_1^i}^2{\lambda_2^i}^2+\overline{D}^2\right], \tag{36a}$$

$$\overline{P}_2 = \lambda_2\left(\chi + \frac{1-\chi}{{\lambda_2^i}^2}\right) - \frac{1}{\lambda_1^2\lambda_2^3}\left[\chi + (1-\chi){\lambda_1^i}^2{\lambda_2^i}^2 + \overline{D}^2\right], \tag{36b}$$

$$\overline{E} = \frac{\overline{D}}{\lambda_1^2\lambda_2^2}. \tag{36c}$$

The inelastic deformation of the material evolves with characteristic time η/μ^{NEQ}. Here we will use it to normalize time t by introducing a dimensionless time, $\tau = t\mu^{NEQ}/\eta$. Upon application of Eq. (33), we may reduce Eq. (25) to the following evolution equations of inelastic stretches:

$$\frac{d\lambda_1^i}{d\tau} = \frac{\lambda_1^i}{3}\left[2\left(\frac{\lambda_1}{\lambda_1^i}\right)^2 - \left(\frac{\lambda_2}{\lambda_2^i}\right)^2 - \left(\frac{\lambda_1^i\lambda_2^i}{\lambda_1\lambda_2}\right)^2\right], \tag{37a}$$

$$\frac{d\lambda_2^i}{d\tau} = \frac{\lambda_2^i}{3}\left[2\left(\frac{\lambda_2}{\lambda_2^i}\right)^2 - \left(\frac{\lambda_1}{\lambda_1^i}\right)^2 - \left(\frac{\lambda_1^i\lambda_2^i}{\lambda_1\lambda_2}\right)^2\right]. \tag{37b}$$

While the method described here is applicable to general cases, in the following discussion, we will look at the special case when the dielectric film is under equi-biaxial stress, such that $\lambda_1 = \lambda_2 = \lambda$, $\lambda_1^i = \lambda_2^i = \lambda^i$, and $\overline{P}_1 = \overline{P}_2 = \overline{P}$. The symmetry of the problem reduces the governing equations (36) to

$$\overline{P} = \lambda\left[\chi + (1-\chi)\lambda^{i^{-2}}\right] - \lambda^{-5}\left[\chi + (1-\chi)\lambda^{i^4} + \overline{D}^2\right],\ \overline{E} = \lambda^{-4}\overline{D}, \tag{38}$$

and (37) to

$$\frac{d\lambda^i}{d\tau} = \frac{\lambda^i}{3}\left[\left(\frac{\lambda}{\lambda^i}\right)^2 - \left(\frac{\lambda^i}{\lambda}\right)^4\right], \tag{39}$$

Some representative solutions to the differential-algebraic system (38) and (39) are plotted in Fig. 2 (a) and (b), for the cases when the film is stress-free, $\overline{P} = 0$, and the applied voltage ramps up linearly with time. The responds to two loading rates are calculated: (a) $d\overline{E}/d\tau = 10$ and (b) $d\overline{E}/d\tau = 0.2$. As initial conditions at $\tau = 0$, the film is fully relaxed with stretches $\lambda = \lambda^i = 1$. The material parameter χ is taken to be 0.5 so that the elastic and inelastic contributions to the free energy are comparable. For the same material, if the voltage is applied at a relatively high rate, the inelastic deformation is small as in Fig. 2 (a), and if at a relatively low rate, the major part of the total deformation is inelastic as in Fig. 2 (b). At the point where the state of the material becomes instantaneously unstable, the deformation rate diverges and the thickness of the film shrinks to 0 instantaneously – a behavior usually referred to as the *pull-in instability* in the context of elastic deformation and equilibrium states. At a higher loading rate, the critical nominal electric field applied is

higher. The critical normalized electric field $\overline{E}_c \approx 0.68$ when $d\overline{E}/d\tau = 10$ is close to that of an elastic material (Zhao et al, 2007a), while the critical normalized field is much lower when the voltage is applied at a relatively low rate. Although the achieved total stretch is larger at a lower loading rate, the elastic stretch which is elastically recoverable, i.e. the difference between the total stretch and the inelastic part, is actually lower. It should also be noted that even though the critical voltage is lower at a lower loading rate, the instantaneous instability still happens later in terms of time.

To study the dependence of the critical conditions for instantaneous instabilities on the inelastic deformation, we explicitly calculate the critical conditions through the determinant of the Hessian. It can be verified that under equi-biaxial stress $\overline{P}$, the critical condition, $\det \aleph = 0$, is equivalent to

$$\overline{D}_c^2 = \overline{E}_c^2 \lambda_c^8 = \frac{1}{3}\lambda_c^6\left[\chi + (1-\chi)\lambda^{i-2}\right] + \frac{5}{3}\left[\chi + (1-\chi)\lambda^{i4}\right]. \tag{40}$$

The critical stretch λ_c is related to the applied nominal stress $\overline{P}$ as, from Eq. (38),

$$\overline{P} = \frac{2}{3}\lambda_c\left[\chi + (1-\chi)\lambda^{i-2}\right] - \frac{8}{3}\lambda_c^{-5}\left[\chi + (1-\chi)\lambda^{i4}\right]. \tag{41}$$

In a special case, either when the material is purely elastic $\chi = 1$ or when the voltage is applied instantaneously so that the material has not deformed inelastically $\lambda^i = 1$, the critical conditions (40) and (41) fully recovers those of an elastic dielectric (Zhao et al, 2007a; Norris, 2007). In general cases, the critical values of the nominal electric field and the stretch are both dependent on the amount of inelastic stretch λ^i, which in turn is highly dependent on the deformation or loading history of the material. Here in order to study the instantaneous stability in the state of interest, we treat λ^i as an input parameter, and plot the critical conditions as functions of it in Fig. 2 (c) and (d).

We first look at the case when no pre-stress is applied, $\overline{P} = 0$. The corresponding critical normalized electric field $\overline{E}_c$ is also plotted in Fig. 2 (d). The dimensionless material parameter χ which characterized the relative significance of the equilibrium polymer network is varied from 0.1 to 0.9. It is clear on Fig. 2 (c) and (d) that for a same material, larger inelastic deformation will lead to a larger critical stretch (though the recoverable stretch is actually smaller), but the critical voltage for instantaneous instability is lower. Accounting for its dielectric strength, a material with low inelastic deformation may experience breakdown before the instantaneous instability at a higher voltage. The result agrees with experimental observations (Plante and Dubowsky, 2006) in which a material loaded at high rate is often subject to electric break down, while it is subject to pull-in instability more often at a lower rate when inelastic deformation is significant.

6.2 Effects of pre-stress

It has been appreciated through experiments that pre-stretching a dielectric elastomer may greatly enhance its actuation performance (e.g. Pelrine et al., 2000a; Pelrine et al., 2000b; Kofod, 2008). The effects have been attributed to the increase in dielectric breakdown strength (Kofod, 2003; Plante and Dubowsky, 2006), the delay in the pull-in instability of an equilibrium state (Zhao et al, 2007a), and the increase in the tangential modulus (Zhao et al, 2007a). Although the effect of the delay after pre-stress on the performance (Plante and Dubowsky, 2006) indicates some viscoelastic property, the pre-stress effects are seldom analyzed in the scope of viscoelasticity.

If both the pre-stress $\overline{P}$ and the voltage are applied instantaneously at the same time, it can be seen by taking $\lambda^i = 1$ in Eqs. (40) and (41) that the critical condition for a viscoelastic dielectric is identical to that of elastic dielectrics (Zhao et al, 2007a; Zhao and Suo, 2007b). However, this limiting case is of less practical importance since the assembly consumes time and the devices shall also have a reasonable lifetime by design. In most applications, pre-stress is applied by stretching the polymer film to a certain level and then fixing it to a semi-rigid frame, and the voltage is applied to an area inside the frame. In contrast to the treatment in some existing analyses (e.g. Zhao and Suo, 2007b), such a setup provides neither constant stress nor constant strain. In fact, the deformation field in the film is highly inhomogeneous. While a detailed numerical analysis is possible by implementing the current theory into finite-element programs, here we introduce the following simplifications to provide a qualitative analysis on the trends. We assume a uniform deformation in the film before a voltage is applied. At $\tau = 0$, an equi-biaxial pre-stretch $\lambda(0) = \lambda_{pre}$ is applied instantaneously to the film. During the interval between the pre-stretch and the application of electric field, the dielectric-elastomer film relaxes under the constant stretch λ_{pre}: the stress $\overline{P}$ decreases while the inelastic stretch λ^i increases, as shown in Fig. 3 (a) and (b). At $\tau = \tau_0$, a voltage is applied with a relatively high rate, $d\overline{E}/d\tau = 10$. In this stage, we still assume the region where the voltage is applied undergoes a homogeneous deformation, and the surrounding region provides a constant nominal traction $\overline{P}$ to the boundaries.

Under these assumptions, the governing equations (38) and (39) are still applicable to the actuated region. Using material parameter $\chi = 0.5$, we solve Eqs. (38) and (39) under three levels of pre-stretches, with $\lambda_{pre} = 1$, 2, and 3, and plot the solutions in Fig. 3 (a) for the short delay case ($\tau_0 = 0.05$) and (b) for the long delay case ($\tau_0 = 2$). To enable comparison, all stretches are normalized by the initial stretches and plotted as λ/λ_{pre}. The solutions are plotted from the application of voltage to the point of instantaneous instability. The onsets of the instability, evaluated directly using the Hessian in Eqs. (40) and (41), are marked with "×" in the figures. When no pre-stretch is applied, $\lambda_{pre} = 1$, the solution recovers that of the stress-free case in Fig. 2 (a). Upon pre-stretching, the performance of the dielectric film is enhanced regardless of the relaxation time, in the sense that a larger actuation strain can be achieved under the same normalized electric field, and the instantaneous (pull-in) instabilities are delayed in terms of actuation strain. However, a marked difference is shown

between the cases of short and long relaxations. The enhancement of the pre-stretch followed by short relaxation approximately doubles that of the same pre-stretch but with long relaxation. If we further look at only the elastically recoverable part of the stretch, $\lambda^e = \lambda / \lambda^i$, the performance of the materials after long relaxation will be diminished even more, since a significant part of the actuation stretch is irreversible. This trend agrees with experimental observations (Plante and Dubowsky, 2006). According to the current model, the negative effect of delay between pre-stretch and loading is mainly due to two mechanisms: the relaxation of membrane stress and the buildup of inelastic deformation. The difference shown in Fig. 3 is the response of a material with parameter $\chi = 0.5$. For a material that is more fluid-like, the dependence on the relaxation time is expected to be more prominent.

6.3 Dynamic response to a cyclic load

As a final example for the usage of the model, we study the dynamic responses of a dielectric elastomer film to a cyclic electric field. Although the level of pre-stress, the payload, as well as the method of clamping all affect the dynamic property of a dielectric elastomer, for the purpose of demonstration and qualitative prediction, we will stipulate the homogeneous assumption and study only the special case when the film is stress-free.

Writing the normalized electric field into a sinusoidal function, $\overline{E} = \overline{E}_0 \sin \omega\tau$, with ω being the dimensionless frequency, one could easily evolve the inelastic stretch λ^i and the total stretch λ by integrating Eqs. (38) and (39) numerically. A set of representative results are presented in Fig. 4. In the solutions plotted, the amplitude of the nominal electric field $\overline{E}_0$ is set to be 0.5, so that the material is not subject to instantaneous instability within the selected frequency range.

When the elastomer is driven by an AC voltage at a relatively high frequency, its deformation would keep in phase with the electric field but the actuation strain is relatively small, as shown in Fig. 4 (a). During the cyclic load, since the actuation strain only depends on the magnitude of the voltage applied, the frequency of the stretch doubles that of the electric field, and the mean value of stretch drifts away from the initial equilibrium state. The inelastic deformation, shown with dashed curves, evolves almost randomly at a short time scale, but approaches at a relatively large time scale to a level which approximately equals the mean stretch. On the trajectory plots of $\overline{E} - \lambda$ and $\overline{E} - \overline{D}$ in Fig. 4 (b) and (c) respectively, no clear limit cycle is shown, and the system shows insignificant hysteresis. Besides the inelastic deformation caused by the average effect of the AC electric field, the response of the elastomer to a high-frequency cyclic load is similar to that of an elastic dielectric.

When the driving voltage alternates at an intermediate frequency, the stretch stabilizes in 1~2 cycles as in Fig. 4 (d). The total stretch λ and the inelastic stretch λ^i are both sinusoidal functions of time approximately. While the amplitude of inelastic stretch λ^i is still markedly smaller than that of λ, the two are now comparable. Limit cycles appears after a few cycles on both the $\overline{E} - \lambda$ and $\overline{E} - \overline{D}$ plots in Fig. 4 (e) and (f). Both plots show hysteresis, and the hysteresis loop on the plot between the work-conjugate pair $\overline{E}$ and $\overline{D}$ indicate that significant amount of energy is dissipated during each cycle.

The area in the hysteresis loop provides an estimate on the theoretical limit of the efficiency, but prediction of the actual efficiency of a device requires the knowledge of the payload applied.

When the dielectric elastomer is actuated by a voltage alternating at a relatively low frequency, the magnitude of the cyclic actuation strain is much larger, and the stretch is almost fully inelastic, i.e. $\lambda \approx \lambda^i$, as shown in Fig. 4 (g). Even though the stretch and the applied voltage are in phase with each other, hysteresis loops can still be observed on the $\overline{E} - \lambda$ and $\overline{E} - \overline{D}$ plots in Fig. 4 (h) and (i), especially when the stretch is relatively large. This is mainly due to the geometric nonlinearity introduced by finite deformation. The dynamic system is highly nonlinear, with the output strain far from sinusoidal while the input voltage is still sinusoidal. The asymmetry in the shape of the cyclic function $\lambda(\tau)$ leads to the hysteresis on the $\overline{E} - \overline{D}$ plot, and thus the irreversible energy loss in each cycle. Evidently, small-deformation linear viscoelastity should not be directly applied to the case demonstrated here.

Although the $\overline{E} - \lambda$ and $\overline{E} - \overline{D}$ hysteresis loops of a viscoelastic dielectric share some similarities with those of ferroelectric ceramics, they differ in the intrinsic mechanisms and some subsequent behaviors. While ferroelectricity is originated from the nonlinearity in the physical polarization property of the material, the hysteresis in a dielectric elastomer is due to the combined effect of nonlinear geometry and inelastic deformation. Therefore, the hysteresis of a ferroelectric appears even in the relation between true electric displacement and true electric field, while no hysteresis is shown for a dielectric elastomer when plotted in true fields. While the $E - D$ curve of a ferroelectric bends towards the E-axis because of the saturation in polarization, the $\overline{E} - \overline{D}$ curve of a dielectric elastomer bends towards the $\overline{D}$-axis due to finite deformation. On the polarization-electric field hysteresis of a ferroelectric, the maximum difference in polarization between the two branches usually appears near $E = 0$, and the corresponding polarization is often referred to as the spontaneous polarization. By contrast, a dielectric elastomer shows no hysteresis or spontaneous polarization under a low electric field – the hysteresis only appears at higher electric field and finite deformation.

7 Concluding remarks

By integrating a recently formulated theory of deformable dielectrics into the framework of nonequilibrium thermodynamics for continuums, this paper develops a general field theory for the coupled electro-viscoelastic behavior of dielectric elastomers. The field theory inherits the merit of traditional continuum mechanics by having the main framework and field equations material-independent, and some interchangeable material-specific modules that are readily measurable from experiments. The adaptiveness of the theory makes it not only applicable to all existing materials, but to emerging new materials as well. For demonstrative purpose, a simple material law is proposed under the theoretical framework. The material law is further used to study the dynamic responses of a dielectric-elastomer film, as well as the influence of pre-stress. Despite the simplicity of the material model prescribed, some basic phenomena have been explained, and the qualitative predictions agree with existing experiments. Moreover, the stability of a general nonequilibrium state of a viscoelastic

dielectric is studied. The idea of instantaneous instability, analogous to the instability of plastic deformations in crystals, has been introduced and related to an important failure mode which is known as the pull-in instability in dielectric elastomers.

Acknowledgement

The author acknowledges the support from the National Science Foundation through Grant No. CMMI-0900342.

References

Arruda, E. M. and Boyce, M. C. (1993) A three-dimensional constitutive model for the large stretch behavior of rubber elastic materials. Journal of the Mechanics and Physics of Solids 41(2), 389412.

Bar-Cohen, Y. (2002) Electroactive polymers as artificial muscles: A review. Journal of Spacecraft and Rockets 39(6), 822-827.

Bar-Cohen, Y., Ed. (2004) Electroactive Polymer (EAP) Actuators as Artificial Muscles: Reality, Potential and Challenges. SPIE Press Monograph Vol. PM136, SPIE, Bellingham, Washington, ed. 2.

Bar-Cohen, Y. and Zhang Q. M. (2008) Electroactive Polymer Actuators and Sensors. MRS Bulletin 33(3), 173-181.

Bergström, J. S., and Boyce, M. C. (1998) Constitutive modeling of the large strain time-dependant behavior of elastomers. Journal of Mechanics and Physics of Solids 46 (5), 931–954.

Boyce, M. C., Weber, G. C. and Parks, D. M. (1989) On the kinematics of finite strain plasticity. Journal of the Mechanics and Physics of Solids 37(5), 641-665.

Blok, J. and LeGrand, D. G. (1969) Dielectric breakdown of polymer films. J. Appl. Phys. 40, 288.

Carpi, F., De Rossi, D., Kornbluh, R., Pelrine, R., and Sommer-Larsen, P., Ed. (2008) Dielectric Elastomers as Electromechanical Transducers. Elsevier, Amsterdam.

Dorfmann, A. and Ogden, R.W. (2005) Nonlinear electroelasticity. Acta Mechanica 174, 167-183.

Dorfmann, A. and Ogden, R. W. (2006) Nonlinear Electroelastic Deformations, Journal of Elasticity 82, 99-127.

Flory, P. J. (1977) Theory of elasticity of polymer networks. The effect of local constraints on junctions. J. Chem. Phys. 66(12), 5720-5729.

Goulbourne, N. C., Mockensturm, E. M., Frecker, M. (2005) A nonlinear model for dielectric elastomer membranes. ASME Journal of Applied Mechanics 72(6), 899-906.

Haupt, P. (1993) On the mathematical modelling of material behaviour in continuum mechanics. Acta Mechanica 100, 129-154.

James, H. M. and Guth, E. (1943) Theory of the elastic properties of rubber. J. Chem. Phys. 11(10), 455-481.

Kofod, G., Sommer-Larsen, P., Kornbluh, R., and Pelrine, R. (2003) Actuation response of polyacrylate dielectric elastomers. J. Intell. Mater. Syst. Struct. 14, 787-93.

Kofod, G. (2008) The static actuation of dielectric elastomer actuators: how does pre-stretch improve actuation? J. Phys. D: Appl. Phys. 41, 215405.

Kornbluh, R., Pelrine, R., Joseph, J. (1995) Elastomeric dielectric artificial muscle actuators for small robots. Proceedings of the Materials Research Society Symposium 600, 119-130.

Kornbluh, R., Pelrine, R., Pei, Q., Oh, S., Joseph, J. (2000) Ultrahigh strain response of field-actuated elastomeric polymers. Proceedings of Smart Structures and Materials: Electroactive Polymer Actuators and Devices, vol. 3987. SPIE, San Diego, CA, 51-64.

Lau, G. K., Goosen, J. F. L., van Keulen, F., French, P. J., and Sarro, P. M. (2006) Actuated elastomers with rigid vertical electrodes. J. Micromech. Microeng. 16, S35-S44.

Lee, E. H. (1969) Elastic plastic deformation at finite strain. ASME Trans. J. Appl. Mech., 36, 1-6.

Lubliner, J. (1985) A model of rubber viscoelasticity. Mechanics Research Communications 12, 93-99.

McMeeking, R. M., Landis, C. M. (2005) Electrostatic forces and stored energy for deformable dielectric materials. J. Appl. Mech. 72, 581-590.

Norris, A. N. (2007) Comment on "Method to analyze electromechanical stability of dielectric elastomers". Appl. Phys. Lett. 91, 061921.

Pelrine, R., Kornbluh, R., Joseph, J. (1998) Electrostriction of polymer dielectrics with compliant electrodes as a means of actuations. Sensor and Actuators A: Physical 64 (1), 77–85.

Pelrine, R., Kornbluh, R., Pei, Q., Joseph, J. (2000a) High speed electrically actuated elastomers with stretch greater than 100%. Science 287, 836-839.

Pelrine, R., Kornbluh, R., and Kofod, G. (2000b) High-strain actuator materials based on dielectric elastomers. Adv. Mater. 12, 1223-1225.

Pelrine, R., Kornbluh, R., Joseph, J., Heydt, R., Pei, Q., Chiba, S., (2000c) High-field deformation of elastomeric dielectrics for actuators. Materials Science and Engineering C 11(2), 89-100.

Plante, J.-S. and Dubowsky, S. (2006) Large-scale failure modes of dielectric elastomer actuators. Int. J. Solids Struct. 43, 7727-7751.

Plante, J.-S. and Dubowsky, S. (2007) On the performance mechanisms of dielectric elastomer actuators. Sensors and Actuators A 137(1), 96-109.

Reese, S. and Govindjee, S. (1998) A theory of finite viscoelasticity and numerical aspects. Int. J. Solids Struct. 35, 3455 3482.

Rice, J. R. (1976) The Localization of Plastic Deformation, in Theoretical and Applied Mechanics (Proceedings of the 14th International Congress on Theoretical and Applied Mechanics, Delft, 1976, ed. W.T. Koiter), Vol. 1, NorthHolland Publishing Co., 207-220.

Richards, A. W. and Odegard, G. M. (2010) Constitutive modeling of electrostrictive polymers using a hyperelasticity-based approach. J. Appl. Mech. 77(1), 014502.

Rinaldi, C., Brenner, H. (2002) Body versus surface forces in continuum mechanics: is the Maxwell stress tensor a physically objective Cauchy stress? Phys. Rev. E. 65, 036615.

Stark, K. H. and Garton, C. G. (1955) Electric strength of irradiated polythene. Nature 176, 1225.

Sugiyama, Y., Hirai, S. (2006) Crawling and jumping by a deformable robot. Int. J. Robot. Res. 25, 603-620.

Suo, Z. G., Zhao, X. H. and Greene, W. H. (2008) A nonlinear field theory of deformable dielectrics. J. Mech. Phys. Solids 56(2), 467-486.

Treloar, L. R. (1975) The Physics of Ruhber Elasticity. Oxford University Press.

Wingert, A., Lichter, M. D., and Dubowsky, S. (2006) On the design of large degree-of-freedom digital mechatronic devices based on bistable dielectric elastomer actuators. IEEE/ASME Trans. Mechatron. 11, 448-456.

Wissler, M., Mazza, E. (2005a) Modeling of a pre-strained circular actuator made of dielectric elastomers. Sensors and Actuators A 120, 184-192.

Wissler, M., Mazza, E. (2005b) Modeling and simulation of dielectric elastomer actuators, Smart Mater. Struct. 14, 1396-1402.

Yang, E., Frecker, M., Morckensturm, E. (2005) Viscoelastic model of dielectric elastomer membranes. Proceedings of Smart Structures and Materials 2005: Electroactive Polymer Actuators and Devices (EAPAD), vol. 5759. SPIE, San Diego, CA, 82–93.

Zeller, H. R. and Schneider, W. R. (1984) Electrofracture mechanics of dielectric aging. J. Appl. Phys. 56, 455.

Zhang, X. Q., Lowe, C., Wissler, M., Jahne, B., and Kovacs, G. (2005) Dielectric elastomers in actuator technology. Adv. Eng. Mater. 7, 361.

Zhao, X. H., Hong, W., and Suo, Z. G. (2007a) Electromechanical hysteresis and coexistent states in dielectric elastomers. Phys. Rev. B 76(13) 134113.

Zhao, X. H. and Suo, Z. G. (2007b) Method to analyze electromechanical stability of dielectric elastomers. Appl. Phys. Lett. 91(6), 061921.

Zhao, X. H. and Suo, Z. G. (2008a) Electrostriction in elastic dielectrics undergoing large deformation. J. Appl. Phys. 104(12), 123530.

Zhao, X. H. and Suo, Z. G. (2008b) Method to analyze programmable deformation of dielectric elastomer layers. Appl. Phys. Lett., 93, 251902.

Zhao, X. H. and Suo, Z. G. (2009) Electromechanical instability in semicrystalline polymers. Appl. Phys. Lett. 95(3), 031904.

Zhou, J., Hong, W., Zhao, X., Zhang, Z., and Suo, Z. (2008) Propagation of instability in dielectric elastomers, Int. J. Solids Struct. 45, 3739-3750.

Figures

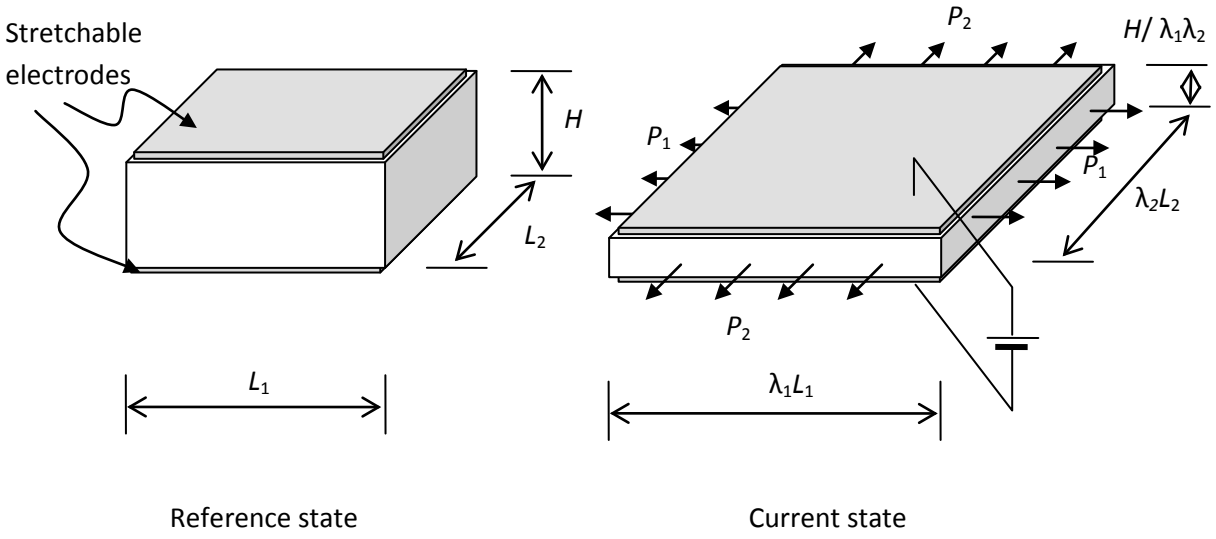

Fig. 1. Sketch of a dielectric-elastomer film deforming uniformly under lateral bi-axial stress and a voltage applied via stretchable electrodes. The elastomer film measures $L_1 \times L_2 \times H$ in the reference state, and $\lambda_1 L_1 \times \lambda_2 L_2 \times H/\lambda_1\lambda_2$ in the current state.

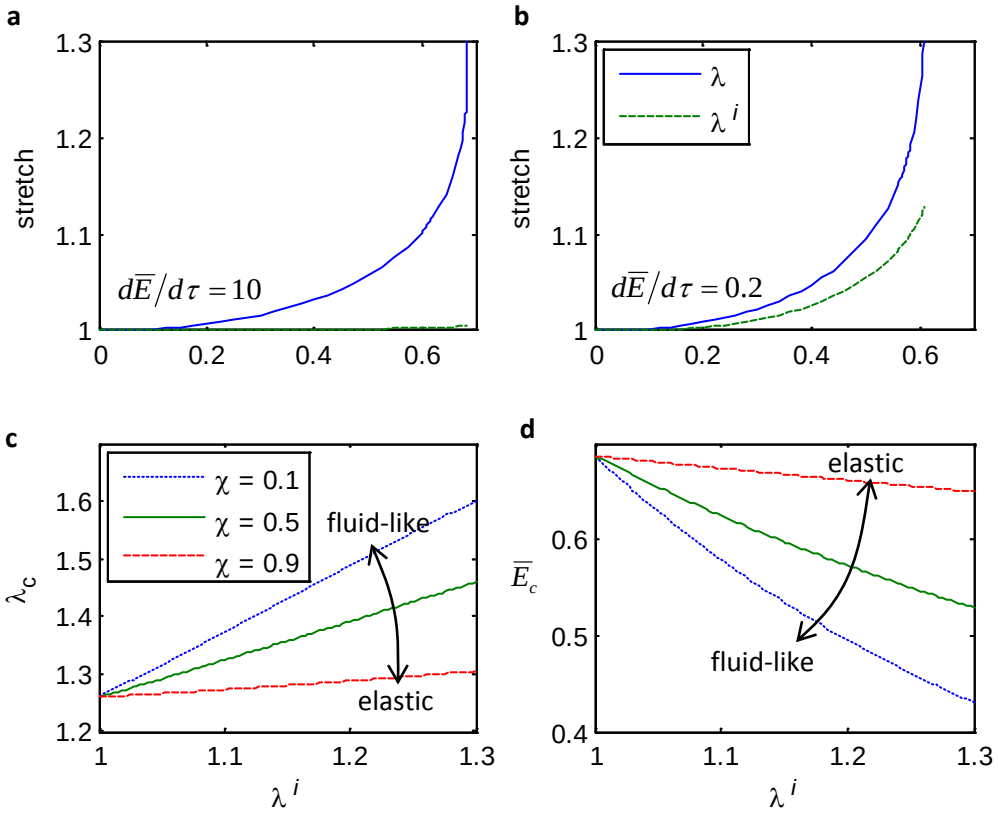

Fig. 2. Evolution of the through-thickness stretch λ (solid curve) and the inelastic stretch λ^i as functions of the normalized applied voltage $\overline{E}$, at a relatively high loading rate (a) and a relatively low loading rate (b). The solutions are plotted up to the points approximately where instantaneous instabilities take place. The critical stretch λ_c (c) and normalized voltage $\overline{E}$ (d) for instantaneous instabilities are plotted as a function of the inelastic stretch λ^i. The responses of three materials with the dimensionless parameter χ ranging from 0.1 (elasticity dominated) to 10 (viscosity dominated) are shown.

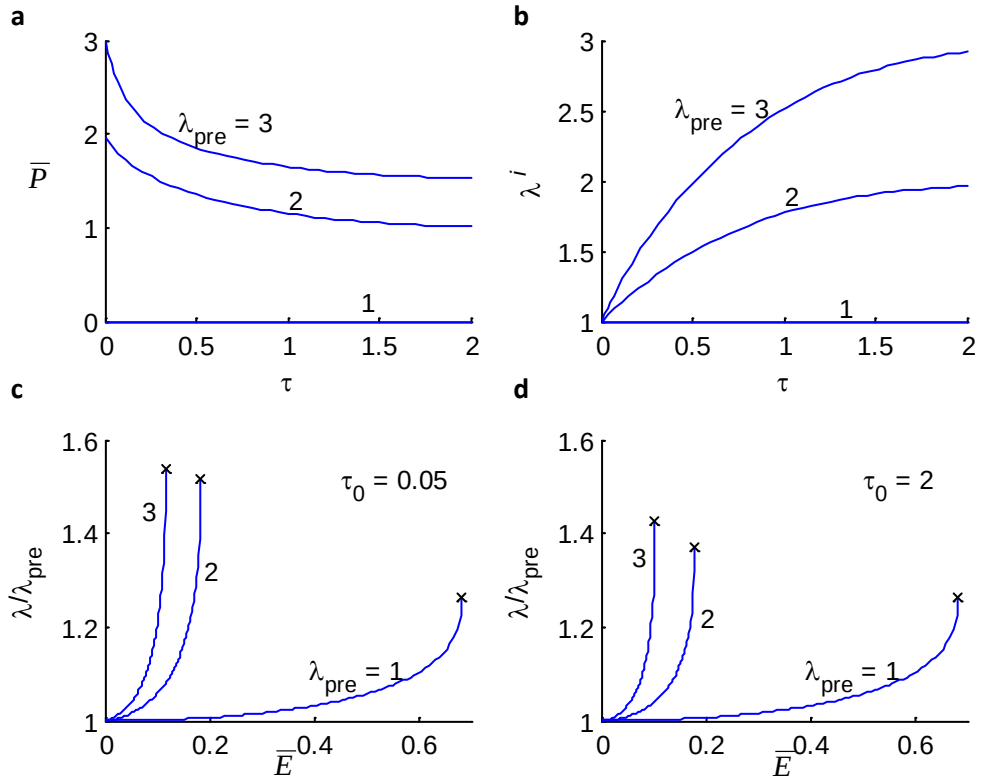

Fig. 3. (a) Relaxation of the dimensionless nominal stress in the film $\overline{P}$ after an equi-biaxial pre-stretch λ_{pre} of various levels is applied instantaneously at $\tau = 0$. The material parameter χ is taken to be 0.5. Therefore, the long-term stress is approximately half of the instantaneous level. (b) Evolution of the in-plane inelastic stretch λ^i after the application of pre-stretch λ_{pre}. (c) Relation between the normalized voltage applied $\overline{E}$ and the in-plane stretch relative to the pre-stretch. The voltage is applied shortly after the pre-stretch, at $\tau_0 = 0.05$. (d) Relation between the normalized voltage and the relative stretch in the case when the film is relaxed for a longer time, $\tau_0 = 2$, before loading. The states of instantaneous instability are marked as "×" in both (c) and (d).

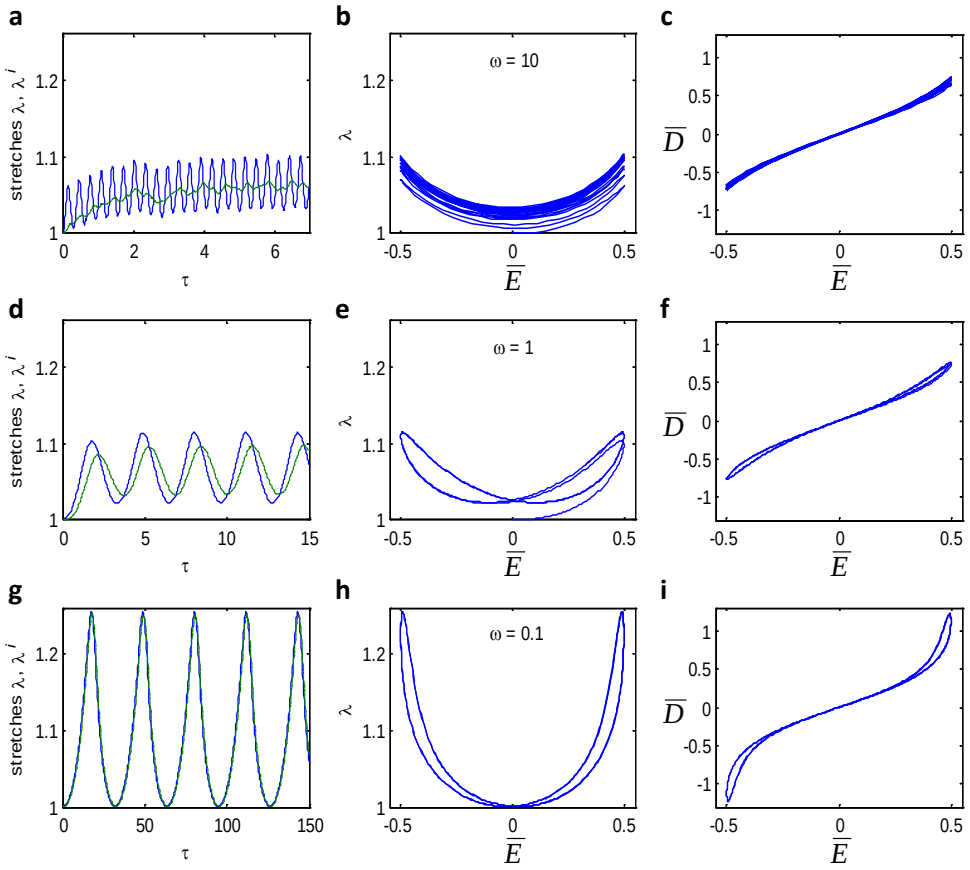

Fig. 4. (a) (d) (g) Total stretch $\lambda(\tau)$ and inelastic stretch $\lambda^i(\tau)$ in a dielectric elastomer film, in response to the applied cyclic nominal electric field, $\overline{E}(\tau)=\overline{E}_0\sin\omega t$. (b) (e) (h) Trajectory plots of the stretch $\lambda(\tau)$ and the applied nominal electric field $\overline{E}(\tau)$ during the process. (c) (f) (i) Trajectory plots of the dimensionless nominal electric displacement $\overline{D}(\tau)$ and nominal electric field $\overline{E}(\tau)$. Three different dimensionless frequencies are used in the calculation: $\omega=10$ for (a-c), $\omega=1$ for (d-f), and $\omega=0.1$ for (g-i).